High fat diet induced liver and kidney damage in hepatocyte specific CBS knockout mouse model, a ROS mediated theory?

HFD INDUCES LIVER STEATOSIS AND ROS IN A HEPATIC CBS-KO MOUSE

Master thesis project of the MSc Pharmacy Program Groningen
Author: T.G. Hendriks
Student number: S2958988
Supervisors:
L.E. Deelman, Department of Clinical Pharmacy and Pharmacology, UMCG Groningen
M. Schmidt, Department of Molecular Pharmacology, University of Groningen
Date: 18-05-2025

Table of contents

Abstract

Non-Alcoholic fatty liver disease (NAFLD) has become one of the leading causes for liver diseases worldwide. More than 30 % of the population is affected by this disease and the numbers are still rising. This illustrates the necessity of more research into the development and treatment of NAFLD to tackle this global burden. In this study we looked into the development of NAFLD in a hepatocyte specific CBS knockout mouse model. Control wildtype mice were able to withstand a high-fat diet without signs of NAFLD such as elevated ALAT levels, ROS production and kidney damage. The CBS knockout animals however showed liver- and kidney damage and increased ROS production when fed a High-fat diet. ROS correlates with ALAT, kidney damage and is therefore likely the main promotor of this HFD induced NAFLD. Since wildtype animals showed no damage when fed a high-fat diet, a beneficial role of hepatic CBS and H_2S is expected in the onset and development of NAFLD. A possible treatment of this disease may be found in the future by further investigation of the role of CBS in NAFLD.

List of abbreviations

Abbreviation	**Meaning**
NAFLD	Non-alcoholic Fatty liver disease
NASH	Non-alcoholic Steatohepatitis
H_2S	Hydrogen Sulphide
CO	Carbon Monoxide
NO	Nitrogen Oxide
ATP	Adenosine Triphosphate
SQR	Sulphide Quinone oxidoreductase
GSH	Glutathione
CBS	Cystathionine beta synthase
CSE	Cystathionine gamma lyase
3-MST	3-mercaptopyruvate sulphur transferase
HHCy	hyperhomocysteinemia
ROS	reactive oxygen species
HFD	High-Fat, High cholesterol Diet
ND	Normal diet
ND12WT	Normal diet 12 weeks Wild type animals
ND12KO	Normal diet 12 weeks CBS knockout animals
HFD12WT	High fat diet 12 weeks Wild type animals
HFD12KO	High fat diet 12 weeks CBS knockout type animals
ND20WT	Normal diet 20 weeks Wild type animals
ND20KO	Normal diet 20 weeks CBS knockout animals
HFD20WT	High fat diet 20 weeks Wild type animals
HFD12KO	High fat diet 20 weeks CBS knockout type animals

Introduction

Recent studies have found an interesting role of dietary methionine in the development of Non-Alcoholic Fatty Liver Disease (NAFLD). Restriction of dietary methionine proved to be beneficial in a murine model[1], where overconsumption may even contribute to the risk of NAFLD.[2] This opens the question to the possible pathways of the onset of NAFLD.

Understanding the pathway of NAFLD is a global necessity, since NAFLD has become one of the most prevalence chronic liver diseases. Latest estimations showed that around 1 in 4 people is affected by this disease.[3 4] NAFLD is an umbrella term for multiple different liver diseases, with the key factor that no overconsumption of alcohol take place. NAFLD first stage is steatosis, where triglycerides accumulate as fatty droplets in more than 5% of the hepatocytes. Both liver size and liver weight increase during steatosis due to the build-up of these fatty droplets. Steatosis is mild and fully reversible by changing diet and lifestyles[5]. However, neglecting steatosis is dangerous and can deteriorate into more severe diseases such as Non-Alcoholic Steatohepatitis (NASH) and Liver cirrhosis. In NASH the fat storage is accompanied with lobular inflammation[6], causing irreversible scar tissue or even hepatocellular carcinoma[7 8]. This scar tissue can eventually develop liver cirrhosis. Prevention of NASH is therefore of great importance. A simplified schematic overview of all the liver diseases is shown in Figure 1.

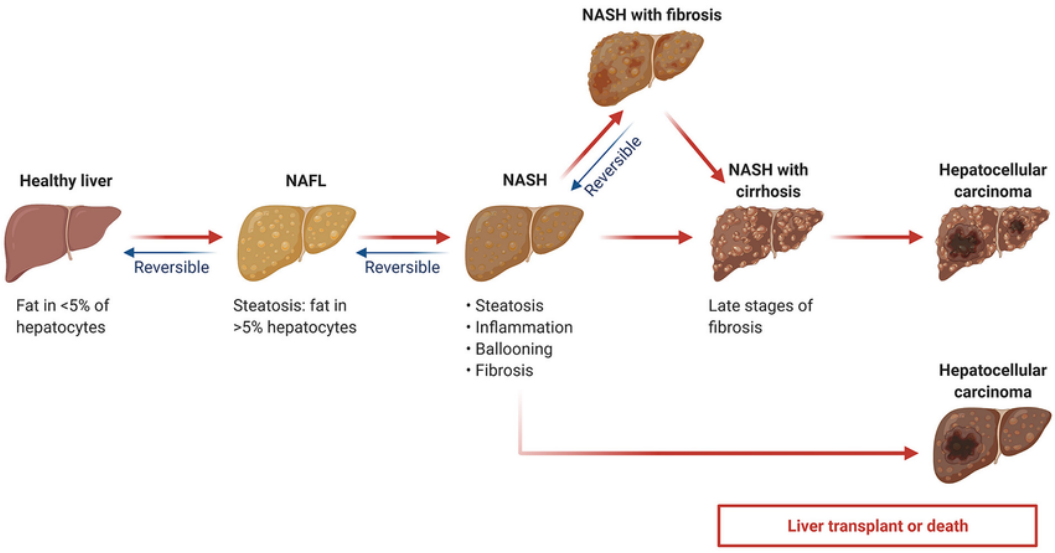

Figure 1 A schematic overview of the different liver diseases such as NAFLD, NASH and hepatocellular carcinoma. **(Wang et al., 2022)[9]**

Beside the forementioned beneficial role of methionine restriction on NAFLD, methionine restriction also leads to elevated Hydrogensulfide (H_2S) production. H_2S is in the past dismissed as a smelly environmental toxic gas. However, H_2S is nowadays a recently found member of the gasotransmitter family, along with Carbon Monoxide (CO) and Nitrogen Oxide (NO). Gasotransmitters are small gaseous signalling molecules. Because of the small molecular size and uncharged appearance, gasotransmitters are capable to rapidly cross cell-membranes through diffusion, making them effective signalling molecules.

H_2S is known to take part in many pathways. The most known is it toxic effect on the mitochondria. This takes place on the electron chain transport on the mitochondria as shown in Figure 2. High levels of H_2S competitively binds to the Cytochrome-C Oxidase (Complex IV) of the mitochondria and therefore inhibit the electron chain and adenosine triphosphate (ATP) production.[10] Interestingly, in lower concentration H_2S can be used as an electron donor to sulfide quinone oxidoreductase (SQR) in the electron chain and therefore helping with the production of ATP.[11] In low concentrations H_2S is also known for its anti-inflammatory effects[12], vasodilative effect on blood vessels[13] and for its role in the anti-oxidant capacity.[14] H_2S scavenges reactive oxygen species (ROS) in different ways. It functions directly as an anti-oxidant, it upregulates anti-oxidants through the Nfr2-AMPK pathway, and H_2S helps with the translocation of glutathione (GSH) into the mitochondria. This suggests a bell-shaped curve for the beneficial and toxic role of H_2S.

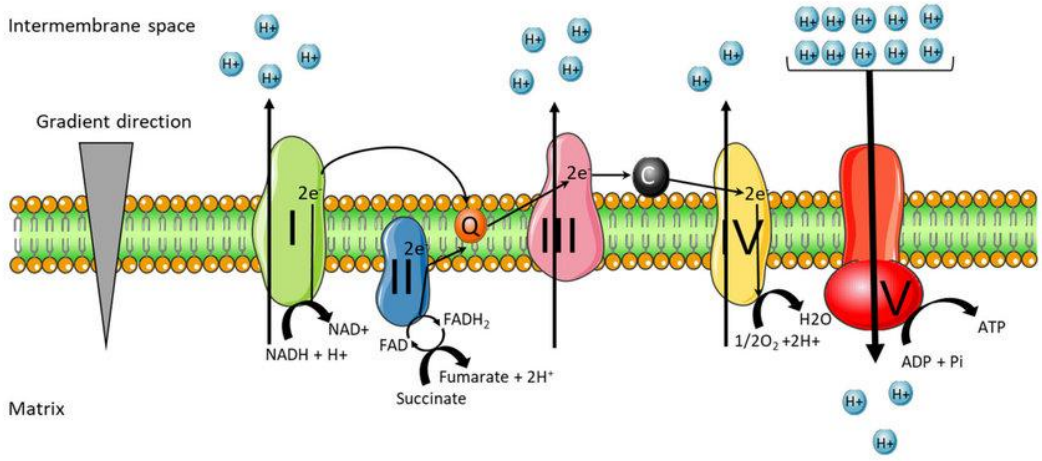

Figure 2 Electron chain transport on intermembrane of a mitochondrium. **(Andrieux et al., 2021)[15]**

H_2S can be formed exogenously by protein degradation and by the microbiome in the gut. Systemic effects of this bacterial derived H_2S are proven[16], yet the exact influence on NAFLD remains unclear. Endogenously, H_2S is produced by enzymatic conversions. Currently there are three enzymes known to produce H_2S; Cystathionine Beta synthase (CBS), Cystathionine gamma lyase (CSE) and 3-mercaptopyruvate sulphur transferase (3-MST). Although all contribute to the synthesis of H_2S, expression levels of these enzymes vary in different tissue. CBS and CSE are known to be the most prevalent H_2S synthesizing enzymes inside the liver.

Beside the production of H_2S, CBS and CSE are also very important in the conversion of homocysteine to cysteine, called the transsulfuration pathway. This pathway is of great importance for the production of glutathione (GSH) and for the production of sulphur containing proteins such as insulin. A simplified schematic overview of this pathway is shown in Figure 3.

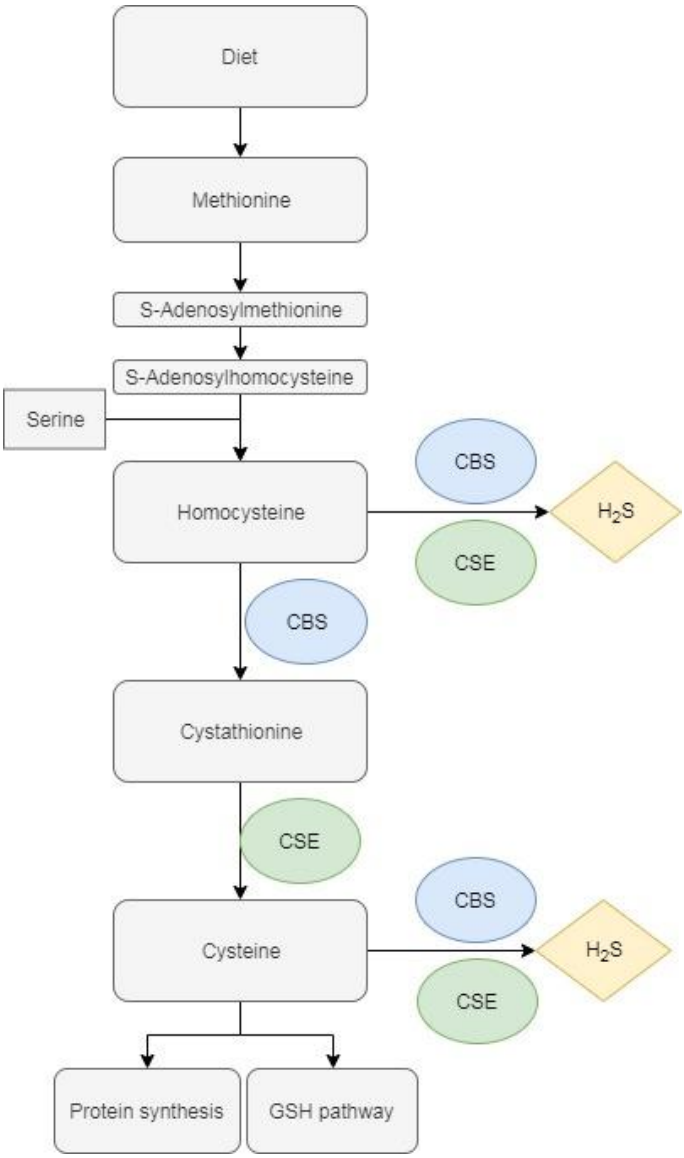

Figure 3 Schematic overview of the enzymatic conversion of methionine to Cysteine by CBS and CSE

Deficiencies in CBS lead to elevated levels of the amino acid homocysteine. This hyperhomocysteinemia (HHCy) takes place, since the conversion to cystathionine is not catalysed anymore. HHCy is a risk factor for different diseases such cardiovascular-, chronic kidney- and Alzheimer's disease.[17] [18] [19] [20]. More interestingly, a number of meta-analyses has shown HHCy is associated with NAFLD.[21] Interestingly, a recent study performed by our lab showed only minor pathology in a mouse model of a whole-body knockout of CBS, despite severe HHCy.[22]

Beside HHCy, also impaired reactive oxygen species (ROS) management is expected with CBS deletion, since CBS is also responsible for the production of compounds for GSH and H_2S production, lowering the total antioxidant capacity. This raised the question whether the total antioxidant capacity has a buffer large enough to withstand CBS deletion and HHCy on itself to maintain ROS homeostasis.

In this study we aim to find a causal relation between impaired ROS handling and CBS deficiency on contrary to HHCy on the development of NAFLD. To investigate HHCy and CBS deficiency, mice models with CBS knockout are already used over 20 years, however many of the mouse models encountered a high mortality rate.[23] To solve the mortality rate, we used a model which inflect the CBS knockout after the embryonic stage. Because our main goal is monitoring the liver, we introduced a hepatocyte specific CBS knockout mouse to create a local deficiency of CBS without interfering with other organs. Since other studies showed that CBS deletion and HHCy on itself are not capable to inflict significant damage, a high-fat, high-cholesterol diet is used to induce high levels of oxidative stress.

Material and Methods

Animals and Diet

All of the animal experiments were approved by the Institutional Animal Care and Use Committee of the University of Groningen, The Netherlands. Methods used in this experiment were conducted in accordance with the relevant guidelines and regulations. Male CBS C57/BL6 with hepatic CBS -/- and CBS +/+ were specially created at the department of Clinical Pharmacy and Pharmacology (K.F.F.) at the University Medical Centre Groningen (UMCG). Hepatic CBS -/- are obtained by selective crossing with homozygous Albumin-Cre. This Cre-Lox system is activated by the production of albumin. Since albumin is only promoted inside the liver, a hepatocyte specific KO is obtained. Wildtype animals were heterozygous for Albumin-Cre, lacking the deletion by Cre. During the early embryonic stage, both knockout and wildtype were still positive for hepatic CBS, since albumin is not yet produced in this stage and therefore the Cre-Lox system not yet activated.

Ten weeks after birth, mice were divided into 8 groups, according to their genotype, diet and time. The diets used in this experiment are a high-fat, high-cholesterol diet (HFD, D14010701) consisting of 60% fat and 0.25% Cholesterol or a normal diet (ND) consisting of regular chow diet. The animals were set on diet for 12 or 20 weeks, after which they were sacrificed.

H_2S measurements

In order to detect H_2S production of CBS in tissue, small volumes of frozen tissue were minced to pieces and mechanically homogenized in 10 times its volume of ice-cold distilled water. The H_2S was analysed by a reaction between lead acetate paper and H_2S to form Lead sulphide, a dark precipitate. 1uL tissue-lysate is added into a 384-well PCR plate together with Cysteine (10mM), Homo-cysteine (2mM), Pyridoxal phosphatase (PLP, 0.25mM) in a HEPES-Buffer (pH 7.4) to a total volume of 10uL. Lead(II)acetate paper, made by soaking and drying a filter paper in a 1 w/w% lead(II)-acetate solution, was placed on top and closed tightly with a lid. After 1 hour incubation in a 5% CO_2 perfused incubator (37℃), pictures were made of the papers using an imager (ChemiDoc MP, Biorad). The intensity of the dark spots was analysed using ImageJ (Fiji). The intensity is inverted and normalized as a percentage of a blank spot of the lead paper.

Western blots

Protein samples for Western blotting were obtained by mincing and homogenizing small pieces of frozen tissue in ice-cold RIPA-buffer modified with proteinase inhibitors (Sodium fluoride (10mM), Sodium orthovanadate (1mM), B-mercapto ethanol(10mM) and 4% v/v protease inhibitor cocktail (c0mplete, Roche, Sigma-Aldrich). Protein levels were determined using Bradford Assay (Biorad). Equal volumes of protein were added to gels (Stainfree TGX mini-Protean, Biorad). Proteins were transferred to a nitrocellulose membrane (Biorad, #1620115) for immunoblotting. After 1 hour blocking in 5% skimmed milk solution in TBST at room temperature, the membranes were incubated overnight with primary antibody (1:1000 in TBST 3% BSA) at 4 ℃. After three times washing for 10 minutes with TBST, membranes were incubated with a secondary HRP-conjugated antibody (1:2000 TBST 3% BSA) for 1 hour at room temperature. Detection took place with ECL-fluid (Western Lighting, PerkinElmer) in combination with an imager (ChemiDoc MP, Biorad). Protein expression is analysed with Imagelab and normalized to total protein concentration of the corresponding lane from the Stainfree image.

Plasma hydrogen-peroxide assay

Frozen plasma was thawed and 100 times diluted in order to measure the hydrogen peroxide concentrations using the Amplex Red® assay (Invitrogen, no. A22188). The assay is performed according to manufactures protocol. The detection was done by a Biotek Synergy H4 platereader.

Plasma ALAT-assay

Alanine transaminase (ALAT) is determined in plasma samples using the Alanine Transaminase Colorimetric Activity assay kit (Cayman chemicals, no. 700260). Frozen plasma is thawed and diluted 2 times with distilled water. The assay is performed according to the manufactures protocol and measured using a Biotek Synergy H4 platereader.

Homocysteine plasma concentration measurement

Homocysteine concentrations in plasma were determined by the clinical laboratory at the University Medical Centre Groningen (UMCG) by a Chemiluminescence Microparticle Immunoassay (CMIA) for homocysteine. KO samples were diluted 25 times with physiologic salt solution before assaying. WT samples were undiluted and were pooled together.

Albumin-creatinine ratio

Urine albumin concentrations were measured using an Albumin ELISA kit (Abcam, ab108792). Urine samples were 100 times diluted in N1X-buffer. The assay is performed according to the manufactures protocol and measured using a plate reader (Biotek Synergy H4). Urine creatinine levels were measured with an enzymatic assay (Creatinine (urinary) Colorimetric Assay Kit, Cayman, No. 500701). Urine samples were 10 times diluted with distilled water according to manufactures protocol. Detection took place using a plate reader (Biotek Synergy H4).

Statistical analysis

Data is analysed using GraphPad prism 8.0. Since the sample size is rather low with a maximum number of 10 samples per group, a test for normal distribution will not produce adequate results. Therefore, an assumption is made that the data of each group is normally distributed. Comparisons between 2 or more groups were performed with an one-way ANOVA (Tukey post hoc). All figures are shown as mean ± SEM. Significant differences are shown with asterisks above the bar, where * =$P<0.05$, ** =$P<0.01$, *** =$P<0.001$ or insignificant (N.S.) $P>0.05$. One asterisk above a bar means that this group is significant to all of the other groups. Correlations are measured by linear regression. When the P-value is smaller than 0.05, a linear regression is seen as significant.

Results

Model confirmation

Western Blot

In order to confirm the hepatic specific CBS -/- model, western blots for CBS were performed on both liver- and kidney tissue of all of the 12-week groups. In the liver CBS protein expression was reduced to almost none in the KO-group on the western blot, while the wildtype group still showed intense bands on the immunoblot as shown in Figure 4A. When the expression is quantified, a significant change is visible in the expression of CBS between knockout and Wildtype animals in the liver, as shown in Figure 4C. This confirms the knockout took place in the liver. To confirm a hepatic specific knockout model, CBS expression is also measured on kidney samples. On this immunoblot, no change is visible between wildtype and knockout as shown in Figure 4B. When this data is quantified, expression levels did not change between the wildtype and knockout mice, confirming the CBS expression did not change in other organs than the liver as shown in Figure 4D.

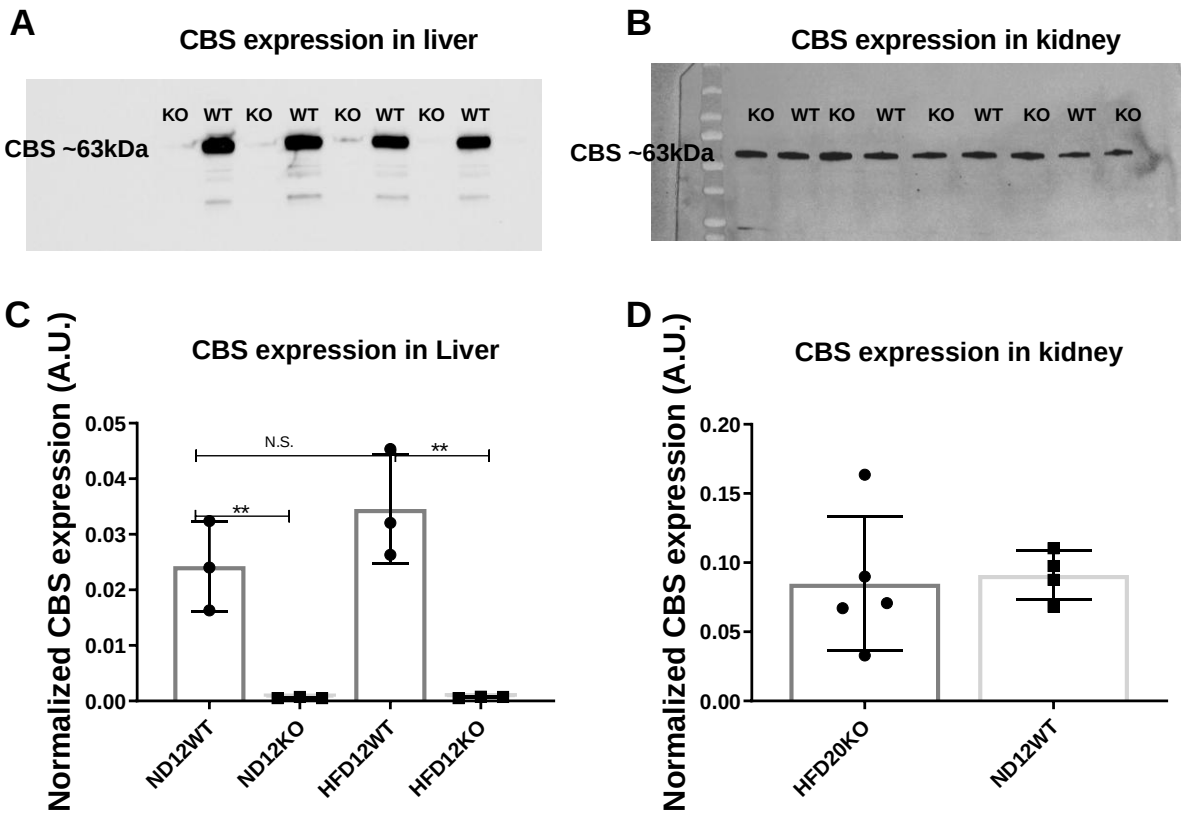

Figure 4 **(A)** Immunoblot of liver protein expression of CBS on knockout and wildtype samples in alternating order **(B)** Immunoblot of Kidney protein expression of CBS on knockout and wildtype samples in alternating order. **(C)** Quantified and normalized CBS expression in liver tissue of different 12-week animal groups. N:3 per group **(D)** Quantified and normalized CBS expression in kidney tissue of HFD20KO and ND12WT groups. N:3 per group. Significant differences are proven by a one-way ANOVA and shown with an asterisk.

H_2S assay

The results of the immunoblots confirmed that a liver specific CBS knock-out has been achieved. Therefore, we aimed to perform a functional assay to confirm the biological activity of the CBS enzyme. To confirm this, a H_2S assay is performed on both liver- and kidney lysate of the animals from the 12-week groups. In Figure 5A is the amount of H_2S produced in liver lysate shown. Wildtype livers produced significantly more H_2S than knockout livers. Interestingly, H_2S production is also significantly increased by HFD relative to the ND in the wildtype livers.

In Figure 5B is the amount of H_2S produced in kidney lysate shown. Both wildtype and knockout animals produced the same amount of H_2S. Both diet and genotype did not change the amount of H_2S produced.

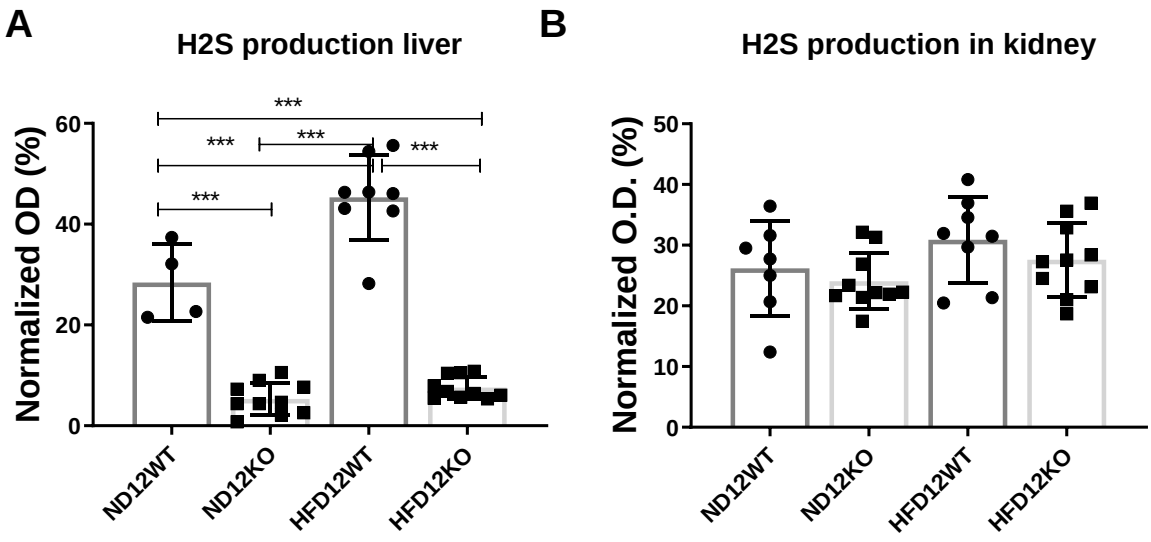

Figure 5 Outcome of H_2S assay with **(A)** liver lysate for ND12WT N:4, ND12KO N:10, HFD12WT N:8 and HFD12KO N:10 **(B)** kidney lysate for ND12WT N:7, ND12KO N:10, HFD12WT N:8 and HFD12KO N:10. Significant differences are proven by a one-way ANOVA and shown with an asterisk.

Hepatic CBS KO results in hyperhomocysteinemia

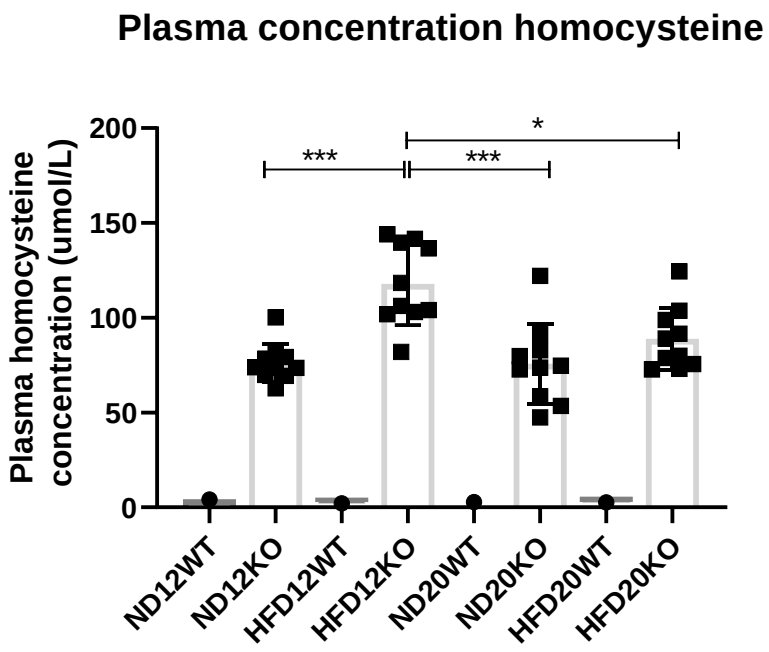

Figure 6 Plasma concentration of homocysteine from all animal groups. WT groups are pooled values of N=7, where KO has individual samples with N=10. Significant differences are proven by a one-way ANOVA and shown with an asterisk.

With the deletion of hepatic CBS, hyperhomocysteinemia is expected. 7 individual samples of wildtype animals were pooled into 1 group to reduce costs. KO animals are measured as individual samples. In the data as shown in Figure 6, confirmation of hyperhomocysteinemia is visible between WT and KO groups. This increase is not statistically proven due to the pooled samples. Interestingly, HFD caused a significant increase on the homocysteine concentrations on 12-week animals, however this is no longer visible at the 20-week animals. The homocysteine levels are lowered on longer exposure of HFD relative to short exposure.

Compensatory mechanisms of H_2S production in the liver

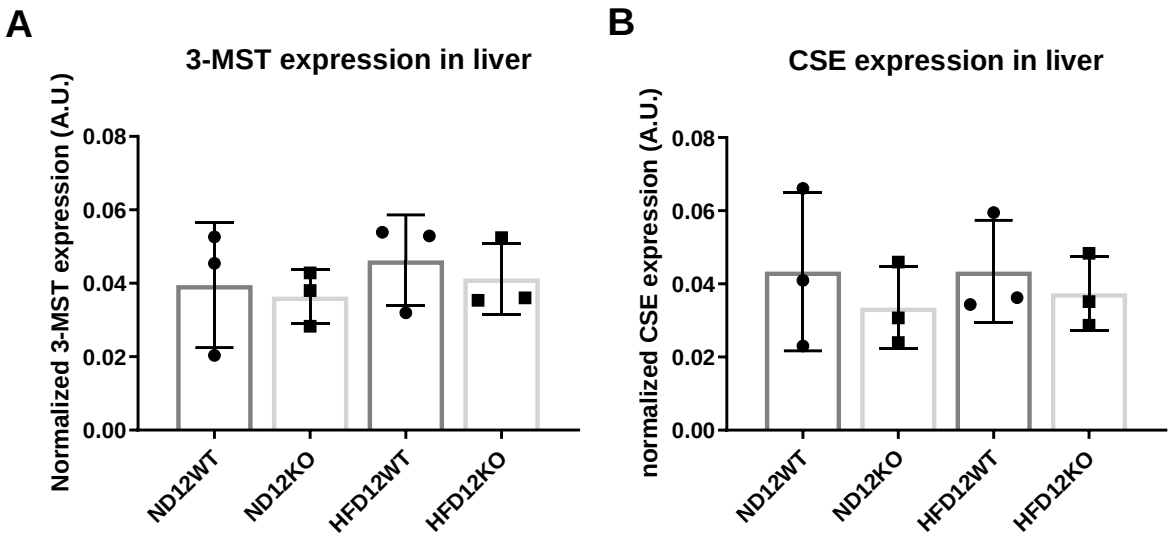

Figure 7 Normalized protein expression of **(A)** 3-MST (N=3 per group) and **(B)** CSE measured by western blot on liver tissue. (N=3 per group)

Since H_2S is produced by 3 enzymes, a homeostatic effect is expected in the other H_2S producing enzymes in the KO animals. To measure this compensatory effect, western blots are performed on liver samples of all the diet groups of all 12-week animals. Interestingly, no compensatory effects are seen for both CSE and 3-MST expression inside the liver.

Organ and bodyweight

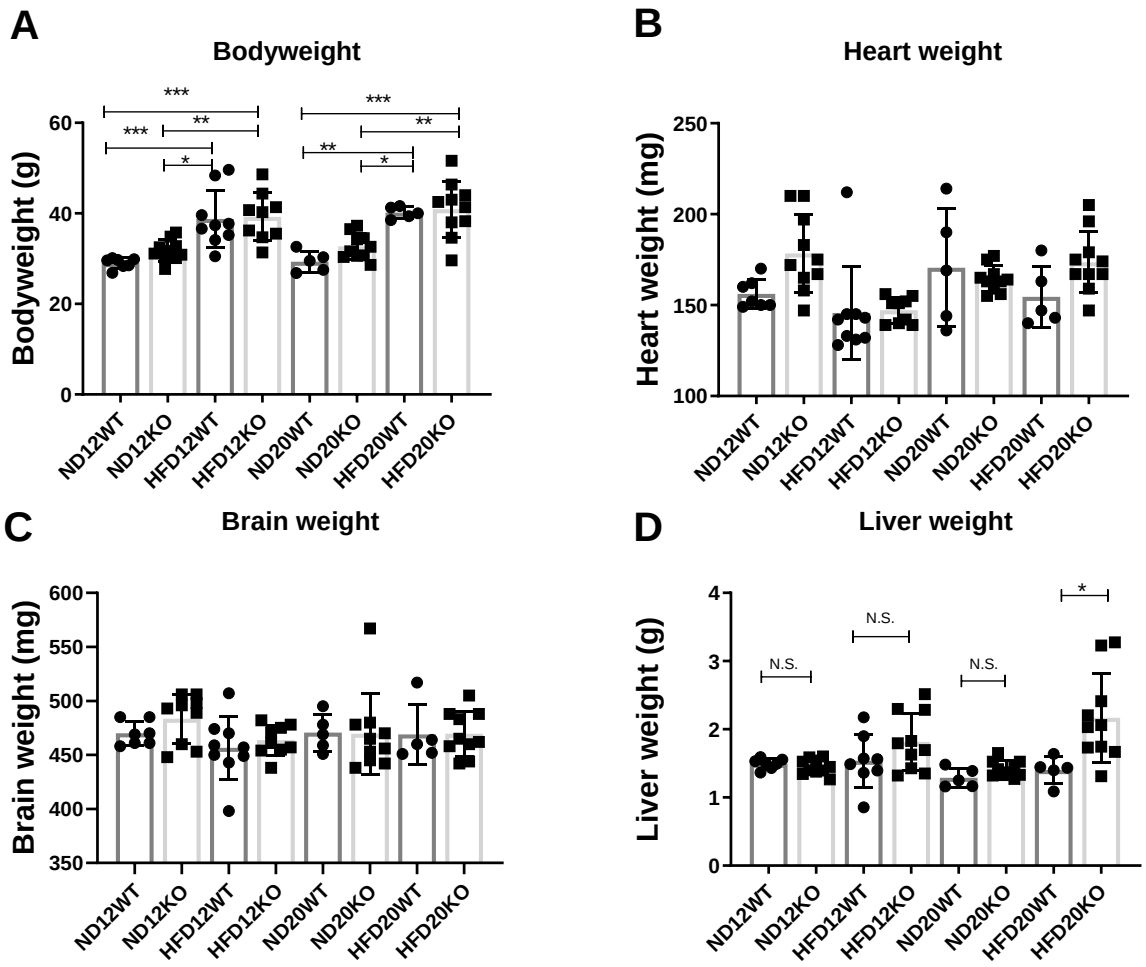

Figure 8 Body- and organ weights in grams of **(A)** Average bodyweight of the experimental groups. **(B)** Average heart weight of the experimental groups. **(C)** Average brain weight of the experimental groups. **(D)** Average liver weight of the experimental groups. Sample size: ND12WT N:7, ND12KO N:10, HFD12WT N:9, HFD12KO N:9, ND20WT N:5, ND20KO N:10, HFD20WT N:5, HFD20KO N:10. Significant differences are proven by a one-way ANOVA and shown with an asterisk.

In order to determine the effects of HFD on the animals, the body weight and organ weight is measured as shown in Figure 8. As expected, HFD increased the body weight significantly in all the animal groups compared to a ND. CBS deletion did not affect the body weight. Although the bodyweight did change, organ weights such as heart and brain did not change under the influences of HFD or CBS deficiency. Only long exposure of 20 weeks of HFD did change the liver weight in the KO group. Interestingly, the distribution between liver weights increases during HFD, implicating individual animals react different on the HFD.

Increased reactive oxygen species in KO animals and HFD

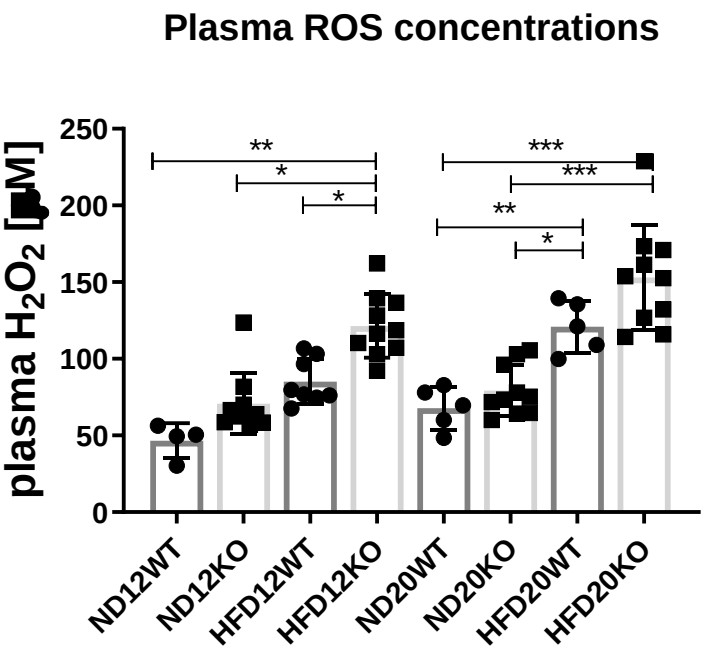

Figure 9 Plasma concentrations of H_2O_2 from the experimental groups. Concentration of H_2O_2 is shown as micromole per liter. Sample size: ND12WT N:4, ND12KO N:10, HFD12WT: N:8, HFD12KO N:10, ND20WT N: 5, ND20KO N:10, HFD20WT N:5, HFD20KO N:10. Significant differences are proven by a one-way ANOVA and shown with an asterisk.

Oxidative stress is analysed by measuring plasma concentrations of H_2O_2 as shown in Figure 9 for all of the experimental groups. As expected, HFD leads to increased ROS levels compared to a ND, however not significantly proven for WT animals on 12-week HFD exposure. An insignificant trend is visible for KO animals having higher ROS levels compared to their WT group. Interestingly, this trend became significant when exposed to HFD for 12 weeks. However, this effect changed again when animals are exposed for 20weeks to a HFD. A levelling effect is visible between the HFD20WT and HFD20KO animals, suggesting long exposure to HFD elevates oxidative stress in a similar way in both genotypes.

Evidence of hepatic damage only in CBS-/- HFD group.

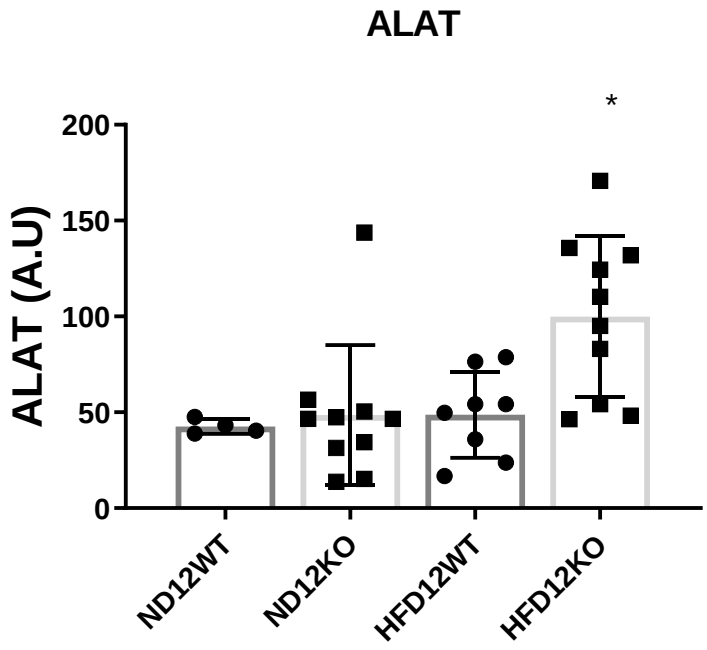

Figure 10 Plasma concentration of ALAT from the 12-week groups. ALAT is displayed in arbitrary units. Sample size: ND12WT N: 4, ND12KO N:10, HFD12WT N:8, HFD12KO N:10. Significant differences are proven by a one-way ANOVA and shown with an asterisk.

Alanine-aminotransferase (ALAT) is a hepatic enzyme. In liver damage ALAT leaks from liver cells into the plasma and therefore is a biomarker of liver damage. ALAT plasma concentrations are measured in 12-week animal groups and shown in Figure 10. Short exposure of HFD diet did not cause liver damage in WT animals, however a significant increase is visible in the HFD12KO group.

Hepatic GSH decreases only with combination of HFD and CBS deletion

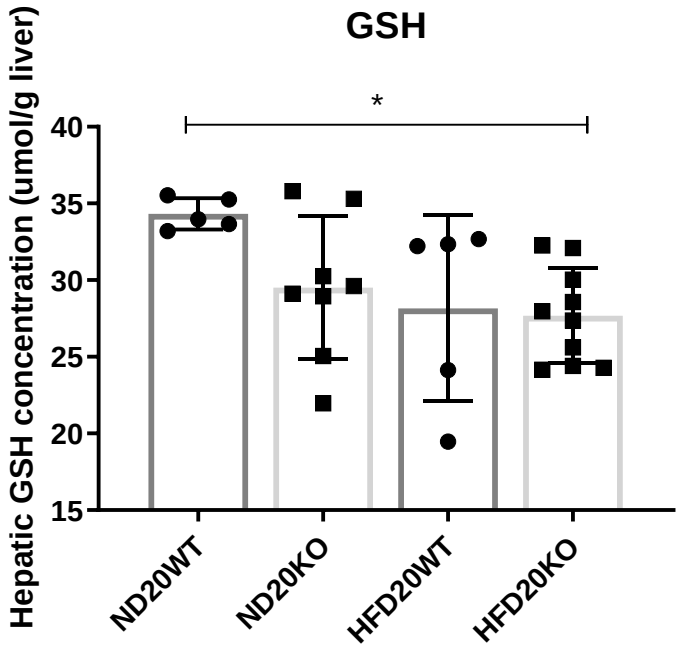

Figure 11 Hepatic GSH concentrations of the 20-week experimental groups. GSH is displayed as micromolar / gram liver tissue. Sample size: ND20WT N:5, ND20KO N:8, HFD20WT N:5, HFD20KO N:10. Significant differences are proven by a one-way ANOVA and showed with an asterisk.

GSH levels are expected to decrease in a CBS KO model. In order to confirm this, hepatic GSH levels were measured and standardized against the amount of liver used as shown in Figure 11. A significant decrease in hepatic GSH is found between the HFD20KO group and the ND20WT group. This suggest HFD or KO on itself is not enough to lower GSH level. However, HFD combined with CBS deletion caused for a decrease in hepatic GSH levels.

Kidney damage

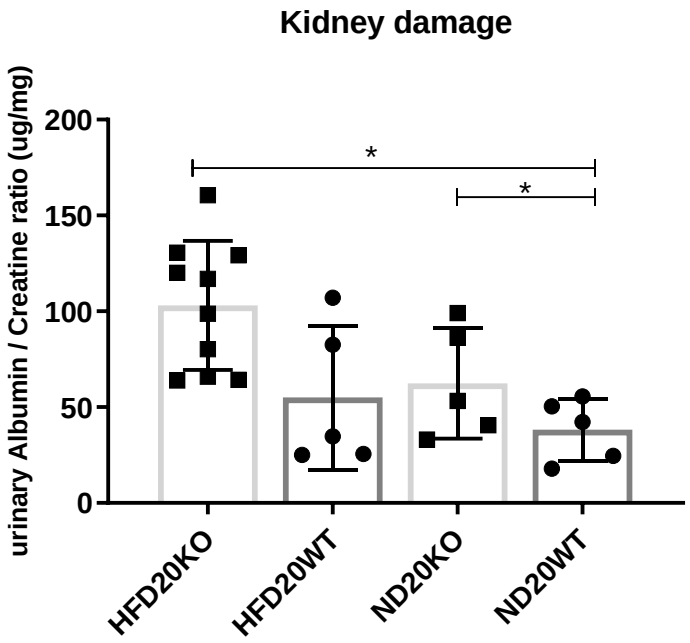

Figure 12 Urinary albumin/creatinine ratios of the 20 weeks experimental groups displayed as microgram Albumin per milligram Creatinine. Sample size: ND20WT N:5, ND20KO N:5, HFD20WT N:5, HFD20KO N:10. Significant differences are proven by a one-way ANOVA and shown with an asterisk.

Urinary albumin / creatinine ratios (ACR) are measured for all of the 20-week groups, as shown in Figure 12. No change is visible between KO and WT animals when fed on ND. HFD did not change the ACR on WT animals on itself, however on KO animals a clear increase is visible in the ACR. This shows neither HFD or CBS deletion on itself is capable of renal damage. However, HFD and CBS deletion will result in renal damage.

Correlations

Liver weight

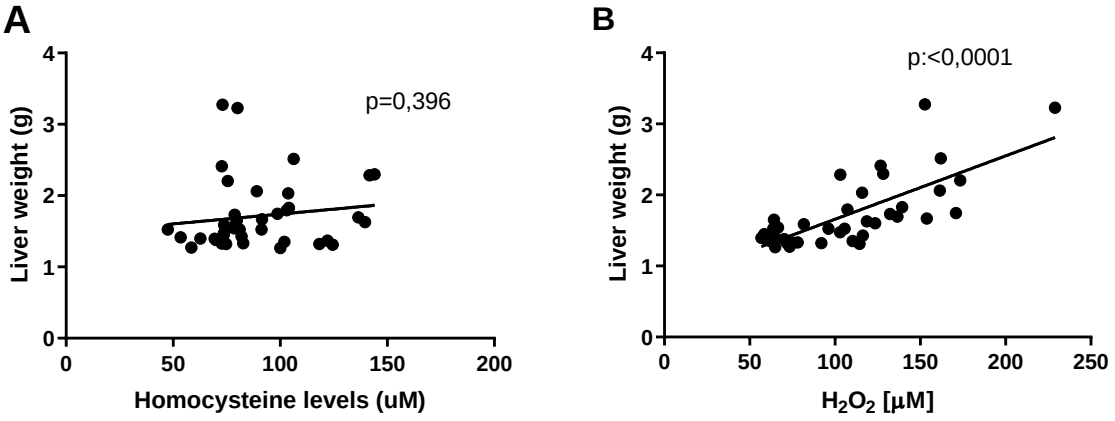

Figure 13 Correlations between all KO animals between **(A)** Liver weight and homocysteine plasma levels Sample size N:40 and **(B)** liver weight and ROS. Sample size N:40.

As shown in Figure 13 Liver weight is correlated with homocysteine and oxidative stress. A clear correlation is found between liver size and plasmatic H_2O_2 concentrations, while no correlation has been found for plasma homocysteine levels.

Kidney damage

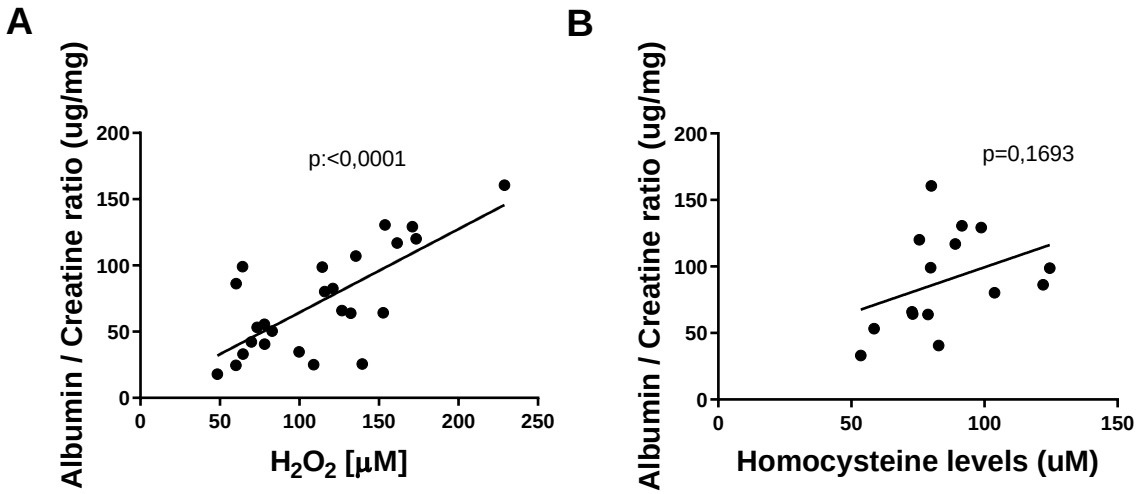

Figure 14 **(A)** Correlation plot of H_2O_2 and Albumin / creatinine ratio with all KO animals Sample size N:25 and **(B)** correlation plot of homocysteine and albumin / creatinine ratio from the 20 weeks knockout animals. Sample size N:15

In Figure 14 are correlations shown between albumin / creatinine ratios and ROS and homocysteine. Interestingly, a clear significant correlation is found between ROS and ACR, while this correlation is not found between ACR and homocysteine levels.

Liver damage

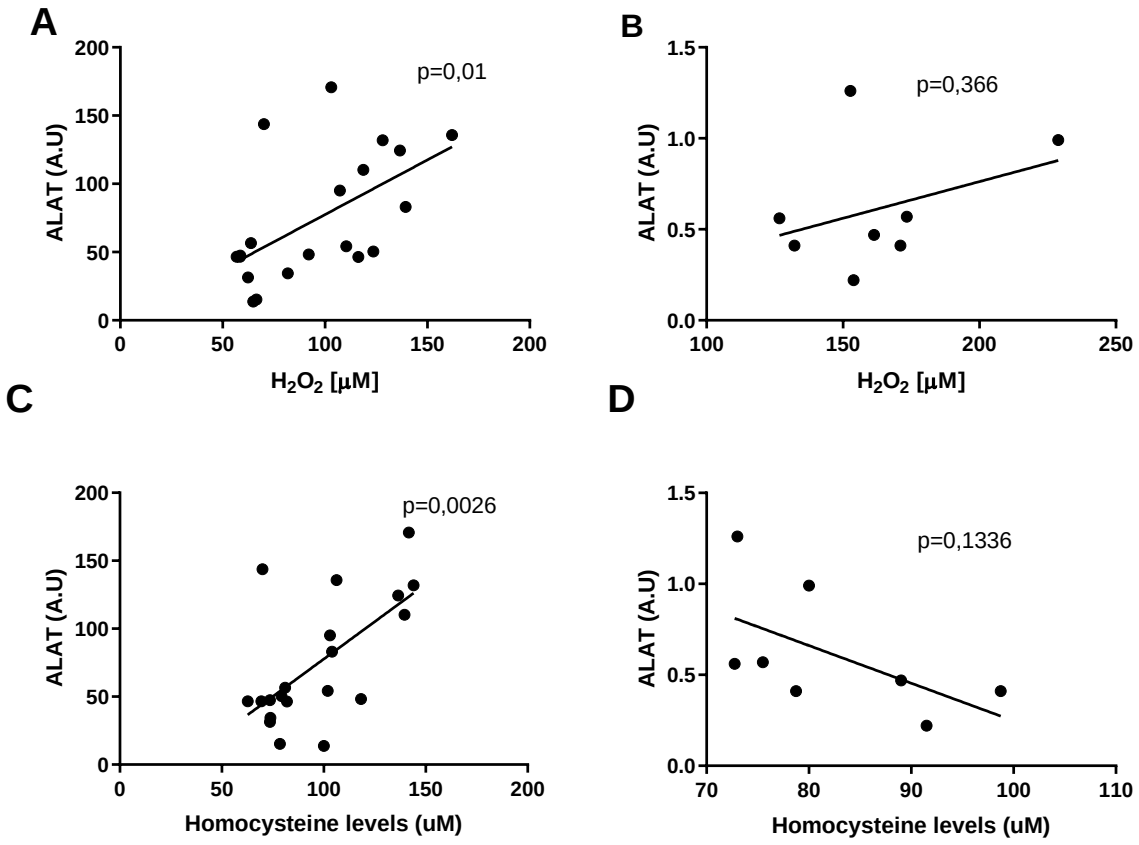

Figure 15 Correlations of ALAT and ROS for 12-weeks knockout animals **(A)** and 20-week knockout animals **(B).** Correlations of ALAT and homocysteine for 12 weeks knockout animals **(C)** and for 20-week knockout animals **(D).**

During the 12 weeks of both ND and HFD, a clear correlation is visible between H_2O_2 levels and the liver damage marker ALAT with a p value of 0,01 as shown in Figure 15A. Higher levels of ROS correlate with higher ALAT concentration in the plasma. During this 12-week diet, homocysteine is also correlating with ALAT, with a p value of 0,003 as shown in Figure15C. So higher levels of homocysteine correlate with higher levels of ALAT. However, when knockout animals are fed for 20 weeks on HFD, ROS does not correlate significantly with ALAT, however the pattern is the same as during the 12-week diet. The pattern of the correlation of homocysteine and ALAT is during the 20 weeks completely different than in the 12-week diet, visible in Figure 15D.

Discussion

Looking at the results we can conclude a couple things. Beginning with the confirmation of our liver specific CBS knockout mouse model. By the results of both the western blots for CBS and the enzymatic H_2S assay on kidney and liver tissue, we can conclude we have successfully created a liver specific CBS mouse knockout model, without changing of other organs such as kidneys. Interestingly, no backup mechanisms were found to maintain homeostasis of H_2S production inside the liver.

Despite CBS was only deficient in the liver, hyperhomocysteinemia is still found inside these animals. This shows the importance of liver CBS in the conversion of homocysteine that even on systemic level no other organ can replace this hepatic deficiency. This buildup of homocysteine suggests a massive decrease in cysteine production and therefore an impaired GSH production. However, under normal conditions, no significant decrease is found in the GSH levels inside the liver. Only during a HFD a significant decrease is found in hepatic CBS. This shows the surplus of the antioxidant capacity. Only during long excessive oxidative stress, a decrease in the GSH is found with CBS deletion.

As expected, HFD caused for a higher body weight in both KO and WT animals. Organ weight such as heart and kidney did not change. Liver weight did significant increase in the HFD20KO group. This means that although the body weight of the KO and WT animals increased the same in HFD, that the liver size did grow more on KO animals. Livers are very regenerative and are able to grow rapidly. It is not sure whether this enlarged liver is a buildup in fatty droplets or that the liver is enlarged by other factors. However, this increase in liver size goes along with liver damage, since HFD12KO showed increased ALAT concentrations. This suggest the enlargement is a bad sign and can be seen as the onset of NAFLD. To conclude this claim, histology should be performed on these liver slices to confirm the build-up of fatty droplets.

Our aim to induce oxidative stress by HFD is proven. Even WT animals showed increase ROS levels during 20 weeks of HFD compared to their control group. This effect is not significantly seen during 12 weeks of HFD, however a trend is already visible. The surplus of GSH is already shown, however this is also visible in the amount of ROS in KO animals. Under ND no change in ROS is found between KO and WT animals for both 12-weeks and 20-weeks experimental groups. However, when exposed to HFD for 12 weeks, a significant increase in H_2O_2 is found in KO animals relative to their control group. Interestingly, this changes during the 20-week exposure. Both KO and WT animals had the same increase in ROS. This means that long exposure of oxidative stress is potent enough to diminish the antioxidant capacity and induce higher concentrations of ROS, even in WT animals.

Since there is a systemic increase of ROS in KO animals under HFD, other damage is expected. This is proven, since urinary albumin / creatinine ratios were increased. This suggests endothelial damage in the kidney. Remarkably this damage is only found in HFD20KO animals, while both animal groups showed he same amount of plasmatic ROS.

While there is a correlation found between ALAT and plasmatic homocysteine for a short exposure of a HFD, this completely changed during long exposure. This suggest the onset of liver damage may be correlated with homocysteine, however the severity of this damage is not correlated on the longer term. The correlation of ALAT and H_2O_2 does correlate on the short exposure, however our test lacks the statistical evidence on the long exposure. Nevertheless, the slope of the correlation is still in the

same direction as on the short exposure, where the correlation with homocysteine changed completely.

All these findings combined suggests a role of elevated ROS-levels in both the onset and severity of liver damage and kidney damage in this mouse model. Looking further into this ROS elevation in liver diseases, research confirms Alcoholic related fatty liver disease is also linked with oxidative- and mitochondrial stress[24]. In alcohol related liver disease, ROS are produced by the metabolism of alcohol. Since both of these diseases are linked with ROS, a possible therapeutic therapy is found in suppletion of antioxidants. A clinical trial has found a beneficial role for Vitamin E in a randomized trial.[25] This confirms the therapeutic role of dosing anti-oxidants as therapeutics for liver diseases.

To dive further in the impaired antioxidant capacity; in our mouse model is a reduction in cysteine / GSH found, because of the impaired conversion from homocysteine by CBS. If this is harmful in the development of NAFLD, a beneficial effect should be found in suppletion with cysteine. This is confirmed by a study were NAFLD patients showed reduced ALAT levels when treated with N-acetylcysteine.[26]

In this mouse model, the ROS was generated by lipid peroxidation by excessive fat in the diet. Reduced lipid concentrations would lead to reduced lipid peroxidation and ROS. This would be beneficial in the development of NAFLD. HMG-CoA reductase inhibitors or statins are widely used medication to reduce cholesterol synthesis. This suggests a beneficial role in the use of statins in the treatment of NAFLD. A meta study confirmed this theory, where statin usage lowered ALAT and cholesterol levels.[27] Another study found a beneficial role of statin in the development of liver fibrosis during NAFLD.[28]

Beside the impaired ROS handling during NAFLD, hepatic and systemic H_2S concentrations are expected to be reduced in this model. This may contribute to the severity of NAFLD, since exogenous H_2S is found to be beneficial in normal mice when on a HFD.[29] Interestingly, recent study showed exogenous H_2S improves NAFLD by inhibition of endoplasmatic reticulum/NLRP3 inflammasome pathway.[30] This illustrates again the versatility and complexity of H_2S in the liver. Since H_2S is also derived from the microbiome, diet and different gut bacteria could be of great importance in the development of NAFLD. However, more research is necessary to confirm this.

Although NAFLD treatment should be prioritized on changing diet and lifestyles, more research into antioxidants, statins, H_2S donors is necessary to tackle this global burden.

Reference

[1] Yang, Y., Wang, Y., Sun, J., Zhang, J., Guo, H., Shi, Y., … Le, G. (2019). Dietary methionine restriction reduces hepatic steatosis and oxidative stress in high-fat-fed mice by promoting H2S production. *Food & Function*, *10*(1), 61–77.

[2] Yang, Y., Lu, M., Xu, Y., Qian, J., Le, G., & Xie, Y. (2022). High dietary methionine intake may contribute to the risk of nonalcoholic fatty liver disease by inhibiting hepatic H2S production. *Food Research International*, *158*, 111507. https://doi.org/10.1016/j.foodres.2022.111507

[3] Younossi, Z. M., Koenig, A. B., Abdelatif, D., Fazel, Y., Henry, L., & Wymer, M. (2016). Global epidemiology of nonalcoholic fatty liver disease-Meta-analytic assessment of prevalence, incidence, and outcomes. *Hepatology*, *64*(1), 73–84. https://doi.org/10.1002/hep.28431

[4] Williams, C. D., Stengel, J., Asike, M. I., Torres, D. M., Shaw, J., Contreras, M., … Harrison, S. A. (2011). Prevalence of Nonalcoholic Fatty Liver Disease and Nonalcoholic Steatohepatitis Among a Largely Middle-Aged Population Utilizing Ultrasound and Liver Biopsy: A Prospective Study. *Gastroenterology*, *140*(1), 124–131. https://doi.org/10.1053/j.gastro.2010.09.038

[5] Centis, E., Marzocchi, R., Di Domizio, S., Ciaravella, M. F., & Marchesini, G. (2010). The Effect of Lifestyle Changes in Non-Alcoholic Fatty Liver Disease. *Digestive Diseases*, *28*(1), 267–273. https://doi.org/10.1159/000282101

[6] Hashimoto, E., Taniai, M., & Tokushige, K. (2013). Characteristics and diagnosis of NAFLD/NASH. *Journal of Gastroenterology and Hepatology*, *28*, 64–70. https://doi.org/10.1111/jgh.12271

[7] Ascha, M. S., Hanouneh, I. A., Lopez, R., Tamimi, T. A.-R., Feldstein, A. F., & Zein, N. N. (2010). The incidence and risk factors of hepatocellular carcinoma in patients with nonalcoholic steatohepatitis. *Hepatology*, *51*(6), 1972–1978. https://doi.org/10.1002/hep.23527

[8] Hashimoto, E., Yatsuji, S., Tobari, M., Taniai, M., Torii, N., Tokushige, K., & Shiratori, K. (2009). Hepatocellular carcinoma in patients with nonalcoholic steatohepatitis. *Journal of Gastroenterology*, *44*(S19), 89–95. https://doi.org/10.1007/s00535-008-2262-x

[9] Wang, H., Sun, R., Yang, S., Ma, X., & Yu, C. (2022). Association between serum ferritin level and the various stages of non-alcoholic fatty liver disease: A systematic review. *Frontiers in Medicine*, *9*. https://doi.org/10.3389/fmed.2022.934989

[10] Cooper, C. E., & Brown, G. C. (2008). The inhibition of mitochondrial cytochrome oxidase by the gases carbon monoxide, nitric oxide, hydrogen cyanide and hydrogen sulfide: chemical mechanism and physiological significance. *Journal Of Bioenergetics And Biomembranes*, *40*(5). https://doi.org/10.1007/s10863-008-9166-6

[11] Szabo, C. (2021). Hydrogen Sulfide, an Endogenous Stimulator of Mitochondrial Function in Cancer Cells. *Cells*, *10*(2), 220. https://doi.org/10.3390/cells10020220

[12] Bourque, C., Zhang, Y., Fu, M., Racine, M., Greasley, A., Pei, Y., … Yang, G. (2018). H 2 S protects lipopolysaccharide-induced inflammation by blocking NFκB transactivation in endothelial cells. *Toxicology and Applied Pharmacology*, *338*, 20–29. https://doi.org/10.1016/j.taap.2017.11.004

[13] Hedegaard, E. R., Gouliaev, A., Winther, A. K., Arcanjo, D. D. R., Aalling, M., Renaltan, N. S., … Simonsen, U. (2015). Involvement of Potassium Channels and Calcium-Independent Mechanisms in Hydrogen Sulfide-Induced Relaxation of Rat Mesenteric Small Arteries. *Journal of Pharmacology and Experimental Therapeutics*, *356*(1), 53–63. https://doi.org/10.1124/jpet.115.227017

[14] Xiao, Q., Ying, J., Xiang, L., & Zhang, C. (2018b). The biologic effect of hydrogen sulfide and its function in various diseases. *Medicine*, *97*(44), e13065. https://doi.org/10.1097/md.0000000000013065

[15] Andrieux, P., Chevillard, C., Cunha-Neto, E., & Nunes, J. P. S. (2021). Mitochondria as a Cellular Hub in Infection and Inflammation. *International Journal Of Molecular Sciences*, *22*(21), 11338. https://doi.org/10.3390/ijms222111338

[16] Tomasova, L., Dobrowolski, L., Jurkowska, H., Wróbel, M., Huc, T., Ondrias, K., Ostaszewski, R., & Ufnal, M. (2016). Intracolonic hydrogen sulfide lowers blood pressure in rats. *Nitric Oxide*, *60*, 50–58. https://doi.org/10.1016/j.niox.2016.09.007

[17] Boushey, C. J. (1995). A Quantitative Assessment of Plasma Homocysteine as a Risk Factor for Vascular Disease. *JAMA*, *274*(13), 1049. https://doi.org/10.1001/jama.1995.03530130055028

[18] Ganguly, P., & Alam, S. F. (2015). Role of homocysteine in the development of cardiovascular disease. *Nutrition Journal*, *14*(1). https://doi.org/10.1186/1475-2891-14-6

[19] O, K., & Siow, Y. L. (2017). Metabolic Imbalance of Homocysteine and Hydrogen Sulfide in Kidney Disease. *Current Medicinal Chemistry*, *25*(3), 367–377. https://doi.org/10.2174/0929867324666170509145240

[20] Beyer, K., Lao, J., Carrato, C., Rodriguez-Vila, A., Latorre, P., Mataro, M., Llopis, M., Mate, J., & Ariza, A. (2004). Cystathionine Beta Synthase as a Risk Factor for Alzheimer Disease. *Current Alzheimer Research*, *1*(2), 127–133. https://doi.org/10.2174/1567205043332243

[21] Dai, Y., Zhu, J., Meng, D., Yu, C., & Li, Y. (2016). Association of homocysteine level with biopsy-proven non-alcoholic fatty liver disease: a meta-analysis. *Journal of Clinical Biochemistry and Nutrition*, *58*(1), 76–83. https://doi.org/10.3164/jcbn.15-54

[22] Nakladal, D., Lambooy, S. P. H., Mišúth, S., Čepcová, D., Joschko, C. P., Van Buiten, A., Goris, M., Hoogstra-Berends, F., Kloosterhuis, N. J., Huijkman, N., Van de Sluis, B., Diercks, G. F., Buikema, J. H., Henning, R. H., & Deelman, L. E. (2022). Homozygous whole body Cbs knockout in adult mice features minimal pathology during ageing despite severe homocysteinemia. *˜The œFASEB Journal*, *36*(4). https://doi.org/10.1096/fj.202101550r

[23] Watanabe, M., Osada, J., Aratani, Y., Kluckman, K., Reddick, R., Malinow, M. R., & Maeda, N. (1995). Mice deficient in cystathionine beta-synthase: animal models for mild and severe homocyst(e)inemia. *Proceedings Of The National Academy Of Sciences*, *92*(5), 1585–1589. https://doi.org/10.1073/pnas.92.5.1585

[24] Tan, H. K., Yates, E., Lilly, K., & Dhanda, A. D. (2020). Oxidative stress in alcohol-related liver disease. *World Journal Of Hepatology*, *12*(7), 332–349. https://doi.org/10.4254/wjh.v12.i7.332

[25] Sanyal, A. J., Chalasani, N., Kowdley, K. V., McCullough, A., Diehl, A. M., Bass, N. M., Neuschwander-Tetri, B. A., Lavine, J. E., Tonascia, J., Unalp, A., Van Natta, M., Clark, J., Brunt, E. M., Kleiner, D. E., Hoofnagle, J. H., & Robuck, P. R. (2010). Pioglitazone, Vitamin E, or Placebo for Nonalcoholic Steatohepatitis. *New England Journal Of Medicine*, *362*(18), 1675–1685. https://doi.org/10.1056/nejmoa0907929

[26] Khoshbaten, M., Aliasgarzadeh, A., Masnadi, K., Tarzamani, M. K., Farhang, S., Babaei, H., Kiani, J., Zaare, M., & Najafipoor, F. (2010). N-acetylcysteine improves liver function in patients with non-alcoholic Fatty liver disease. *PubMed*. https://pubmed.ncbi.nlm.nih.gov/22308119

[27] Dai, W., Xu, B., Li, P., & Weng, J. (2022). Statins for the Treatment of Nonalcoholic Fatty Liver Disease and Nonalcoholic Steatohepatitis: A Systematic Review and Meta-Analysis. *American Journal Of Therapeutics*, *30*(1), e17–e25. https://doi.org/10.1097/mjt.0000000000001499

[28] Lee, J. I., Lee, H. W., Lee, K. S., Lee, H. S., & Park, J. (2020). Effects of Statin Use on the Development and Progression of Nonalcoholic Fatty Liver Disease: A Nationwide Nested Case-Control Study. *The American Journal Of Gastroenterology*, *116*(1), 116–124. https://doi.org/10.14309/ajg.0000000000000845

[29] Wu, D., Zheng, N., Qi, K., Cheng, H., Sun, Z., Gao, B., Zhang, Y., Pang, W., Huangfu, C., Ji, S., Xue, M., Ji, A., & Li, Y. (2015). Exogenous hydrogen sulfide mitigates the fatty liver in obese mice through improving lipid metabolism and antioxidant potential. *Medical Gas Research*, *5*(1), 1. https://doi.org/10.1186/s13618-014-0022-

[30] Fu, X., Zhang, Q., Chen, Y., Li, Y., & Wang, H. (2025). Exogenous hydrogen sulfide improves non-alcoholic fatty liver disease by inhibiting endoplasmic reticulum stress/NLRP3 inflammasome pathway. *Molecular And Cellular Biochemistry*. https://doi.org/10.1007/s11010-025-05220-3

Appendix

Western Blot

CBS

Liver

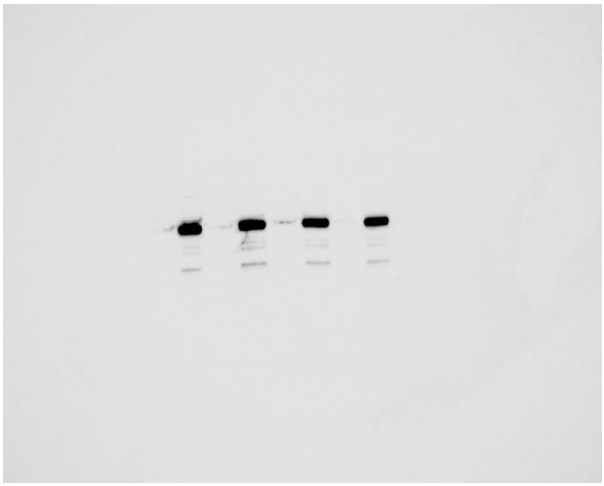

Appendix 1 Chemiluminescent picture of Western Blot of CBS of liver lysate. In alternating order is visible HFD20KO and ND12WT.

Kidney

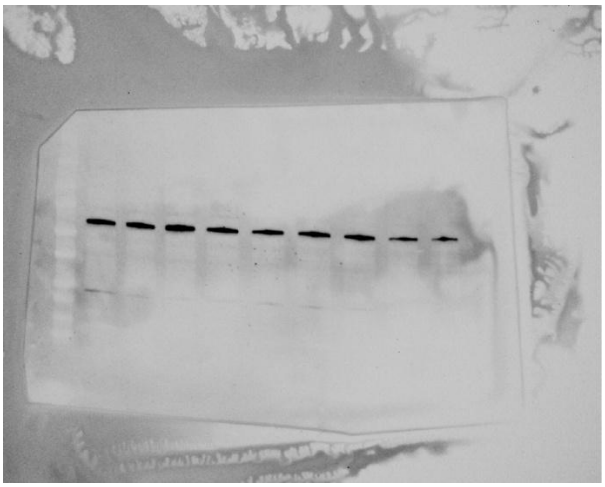

Appendix 2 Chemiluminescent picture of Western Blot of CBS of kidney lysate. In alternating order is visible HFD20KO and ND12WT.

CSE

Appendix 3 Chemiluminescent picture of Western Blot of CSE of liver lysate. Lane 1 to 5 consists of HFD20KO. Lane 6 to 9 consists of ND12WT.

3-MST

Appendix 4 Chemiluminescent picture of Western Blot of 3-MST of liver lysate. Lane 1 to 5 consists of HFD20KO. Lane 6 to 9 of ND12WT.

H_2S assay

Liver

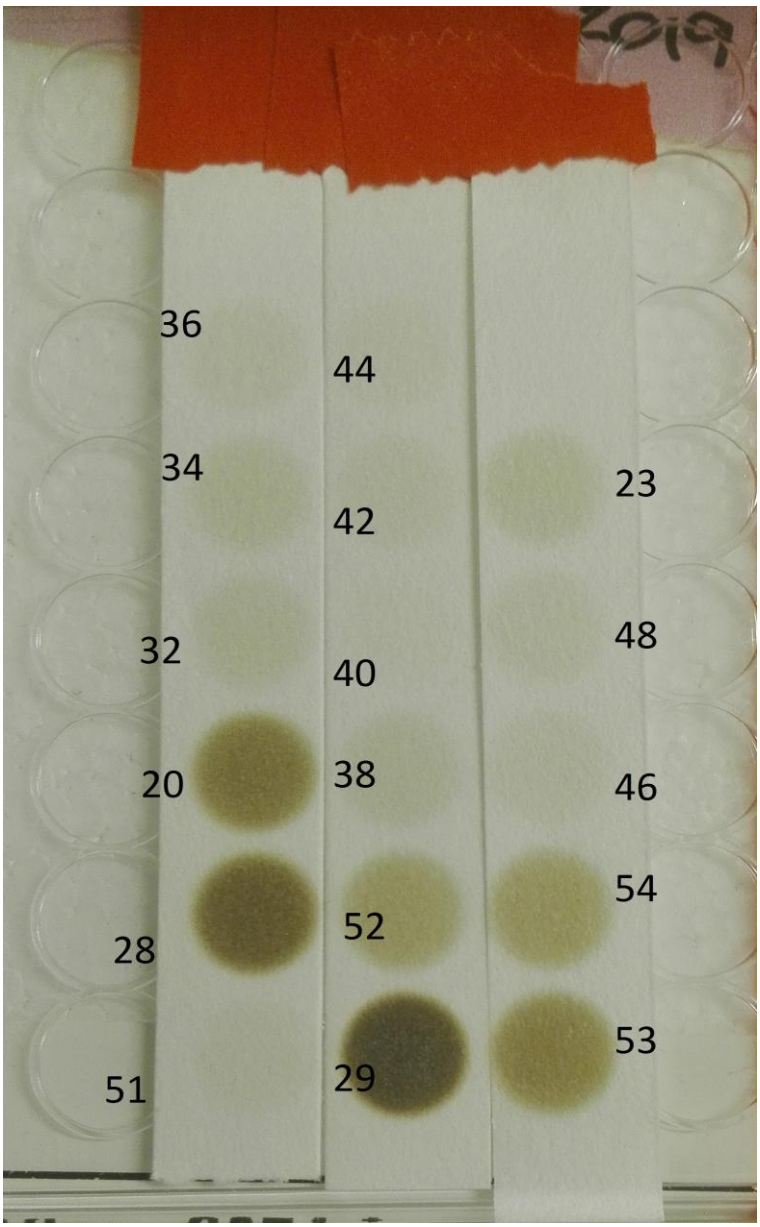

Appendix 5 Outcome of a H_2S assay on liver lysate. Numbers 23, 32, 34, 36, 38, 40, 42, 44, 46 and 48 are HFD12KO. Numbers 20, 52, 53 and 54 are ND12WT. Number 51 is ND12KO and numbers 28 and 29 are HFD12WT

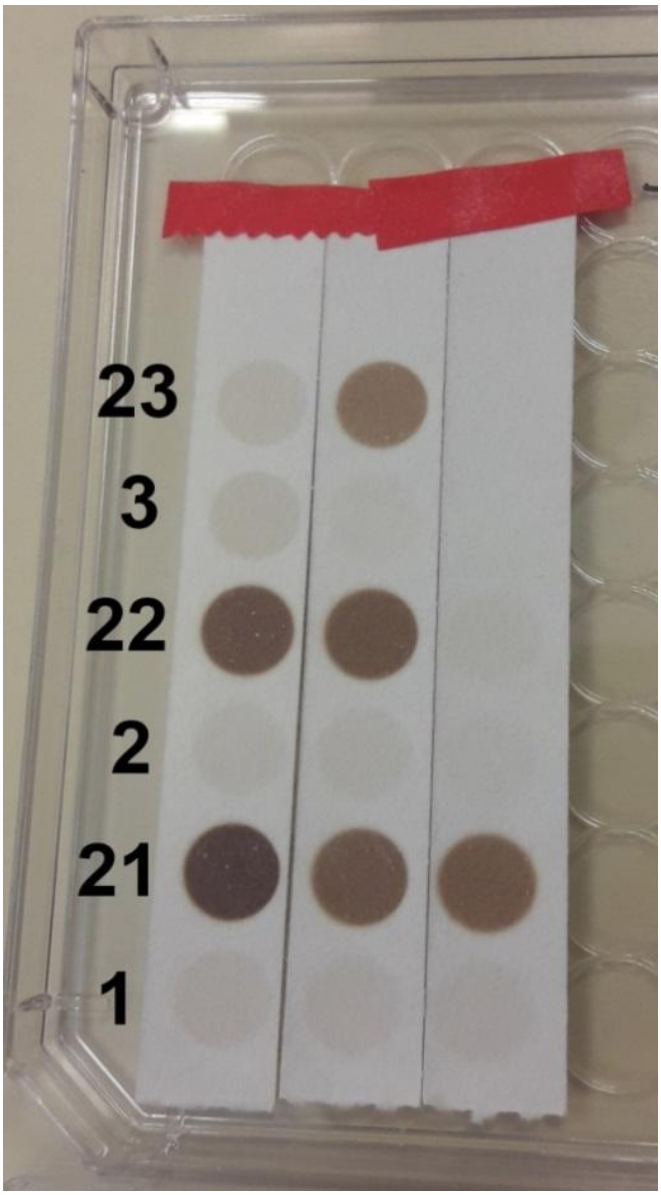

Appendix 6 Outcome of a H_2S assay on liver lysate. Numbers 1, 2 and 3 are ND12KO. Numbers 21 and 22 are HFD12WT. Number 23 is HFD12KO

Kidney

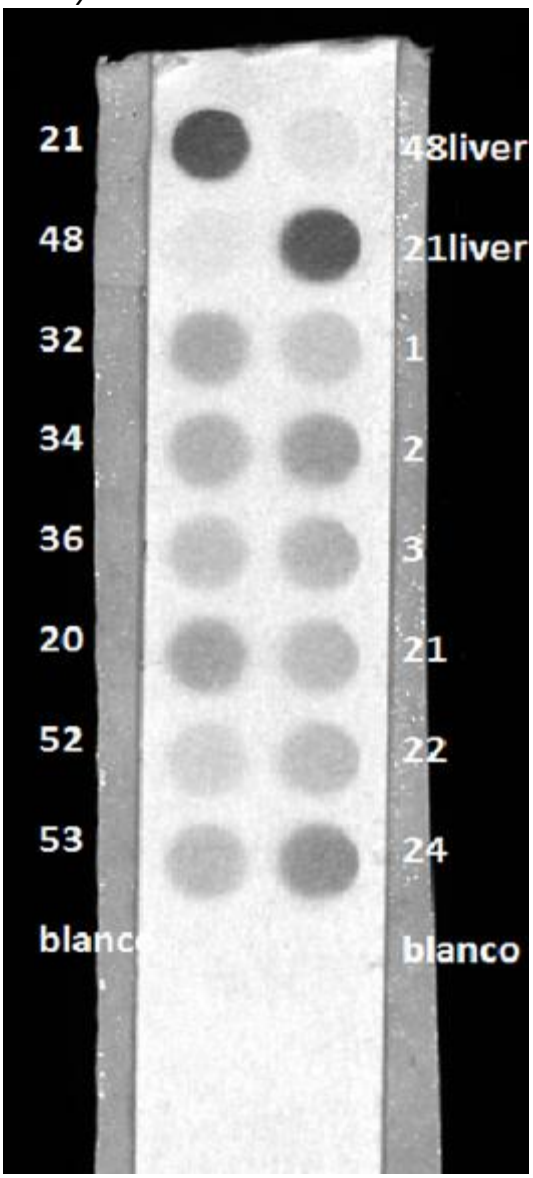

Appendix 7 Outcome of H_2S assay on kidney lysate. Numbers 32,34,46 are HFD12KO. Numbers 20, 52, 53 are ND12WT. Numbers 1, 2, 3 are ND12KO. Numbers 21, 22, 24 are HFD12WT. Numbers 21 and 48 are control samples of liver lysate.